Photon absorption of conduction-band electrons and their effects on laser-induced damage to optical materials

Tian-qing Jia,* Hong Chen, and Yu-mei Zhang
Pohl Institute of Solid State Physics, Tongji University, Shanghai 200092, People's Republic of China
(Received 10 June 1999; revised manuscript received 16 December 1999)

The one- and two-photon absorption rates of conduction-band electrons (CBE) in optically transparent materials under the radiation of high-intensity lasers at visible and ultraviolet wavelengths are calculated by the quantum field approach. When both hole-assisted linear absorption and nonlinear absorption of CBE are considered, the rates of total energy gain from the laser field will be enhanced by a factor of 2. The bounding intensity for the avalanche dominating damage process thus decreases by about one-third. The avalanche rate includes not only the term proportional to the laser intensity, but also the terms proportional to the square of the laser intensity and to the product of the laser intensity and hole density. The present result gives a lower damage threshold than previous ones.

I. INTRODUCTION

Ultrashort-pulse lasers are used routinely for micromachining, x-ray generation, relativistic plasma physics, and inertial confinement fusion.[1–3] Compared with infrared light, lasers at visible and ultraviolet (UV) wavelengths can be focused onto smaller areas, and their absorption coefficients in common materials are much higher.[1] Therefore, these lasers are more advantageous for future applications. However, further increases in the peak power available from such laser systems are now limited by laser-induced damage (LID) to optical components.

Laser-induced damage in optically transparent materials has been studied extensively for many years.[4–15] It is believed LID may be described by three major processes:[11] generation of conduction-band electrons (CBE), heating of CBE, and transferring of their kinetic energies to a lattice. Impact ionization and multiphoton absorption are considered as two competitive processes of CBE generation.[5–7] The process of impact ionization, i.e., avalanche, has the following basic picture.[4,5] When the rate of energy gain from laser field exceeds the rate of energy loss in the lattice, the starting electron rapidly accelerates to kinetic energy larger than the forbidden band gap, undergoing impact ionization and CBE multiplication, thus leading to an exponential increase of the CBE density. It is clear from the above picture that the mechanisms and the rates of energy gain by CBE from laser field are two important factors which determine the avalanche processes, and thus determine under what experimental conditions it is avalanche or multiphoton absorption that dominates the CBE generation process. The laser energy absorbed by CBE can be transferred to lattice by phonon scattering, resulting in lattice melting, ablation, or mechanical damage.[9–11] This analysis indicates that the heating process of CBE has a great influence on both the CBE generation and the energy transfer from laser field to lattice. Therefore, the heating process of CBE or the interaction of a high-intensity laser field with CBE plays a crucial role in understanding LID mechanisms and determining the damage threshold.

In connection with the laser-field–CBE interaction, two different methods, i.e., classical approximation and quantum approach, have been adopted.[4–9] In the classical approximation, the laser field is treated as an alternating electric field at the laser frequency, and its quantum nature is neglected.[4,9] CBE kinetic energy changes continuously in time. This approximation fails when the average CBE kinetic energy is small compared with the photon energy, which is the case for short wavelengths. Using both the classical and quantum approaches, Arnold and Cartier calculated the rates of energy gain by CBE from a laser field,[5] where acoustic phonon- and longitudinal optical (LO) phonon-assisted linear photon absorption were considered. The CBE mediated energy transfer from the laser field to the solid is calculated by Monte Carlo simulation of the Boltzmann transport equation. By comparing the CBE average kinetic energy, power transfer, and impact ionization rate obtained by both of the two methods, they found that the classical approach is valid for $\lambda > 2\ \mu$m, while the results obtained using the quantum approach is reliable for short wavelengths, $\lambda < 1\ \mu$m.

The phonon-assisted linear photon-absorption process considered in Ref. 5 is a good description of the laser-field–CBE interaction *only* for the case of long pulse lasers. But for ultrashort pulse lasers, the peak power of the damage thresholds of dielectrics is of the order of TW/cm^2.[7,11–14] Now two factors beyond the phonon-assisted linear process should be taken into account. One is the phonon-assisted nonlinear absorption process, since the rate of multiphoton ionization has been estimated to be very high based on the multiphoton absorption coefficients obtained experimentally and theoretically.[17–19] The other is the hole-assisted photon-absorption process of CBE, since in the latter half of the laser pulses, the density of CBE produced by multiphoton ionization will be of the order of 10^{19}/cm^3 to 10^{20}/cm^3. Unfortunately, both of the two kinds of processes have seldom been investigated.

In this paper, the interaction of a high-intensity laser field at visible and ultraviolet wavelengths with CBE in wide-gap solids is treated by quantum field theory. Besides the rates of phonon-assisted one-photon absorption, the rates of hole-assisted one-photon absorption and two-photon absorption

are also presented as a function of CBE kinetic energy. It is shown that the phonon-assisted nonlinear absorption process contributes greatly to CBE heating under visible laser radiation, while the hole-assisted linear absorption process is very important for uv lasers. Combining these two processes can enhance the rates of CBE energy gains by a factor of 2 and reduce the bounding intensity of avalanche breakdown by about one-third. The dependence of avalanche rate δ on the laser intensity F and hole concentration N_h is studied and we find it contains terms of F, F^2, and FN_h, rather than only the linear term of F. Compared with the case in which only the phonon-assisted one-photon absorption is considered, the present results indicate that the avalanche rates of fused silica under ultrashort laser radiation increase greatly, and so does the density of CBE produced through impact ionization. It was proposed that the multiphoton absorption is the dominant process of CBE production for visible lasers, and the effect of impact ionization is negligible for uv lasers. However, we find it is the impact ionization that dominates the CBE production for ultrashort-pulse visible lasers, and it is also important for uv lasers. When the two processes of CBE energy gains are considered, the damage threshold will be lowered by about 15% for 1 ps pulse width laser, and it will continue to decrease as the laser pulse duration is decreased.

Fused silica is selected as a subject for our numerical calculations for a few reasons. First, a great deal of theoretical and experimental information exists on electron scattering,[20–22] which is important since any prediction about the damage mechanism and damage threshold depends critically on it. Second, these materials are widely used in fine optical components for their excellent optical transmission and smaller thermal expansion.[1,13] Moreover, they are the only amorphous materials that can be used in excimer lasers.

The paper is organized as follows. The one- and two-photon absorption rates are calculated by quantum field theory in Sec. II and Sec. III, respectively. In Sec. IV, the effects of the phonon-assisted nonlinear absorption and the hole-assisted linear absorption on LID processes and damage threshold are discussed. In Sec. V, a brief conclusion is presented.

II. SECOND-ORDER PERTURBATION THEORY

A photon can be absorbed by CBE only if a phonon is simultaneously absorbed or emitted, or CBE is scattered off a hole for energy and momentum conservation, since its momentum is very small.[23] The phonon- and the hole-assisted one-photon absorption rates can be calculated by standard second-order perturbation theory. The interacting Hamiltonian is[24]

$$H = H_{eL} + H_{eh} + H_{ep}, \tag{1}$$

$$H_{eL} = \sum_{k,\nu} \frac{-\hbar e}{m}\sqrt{\frac{\hbar}{2\omega_\nu \varepsilon_\nu}}\vec{a}\cdot\vec{k}[c^+_{k+\nu}c_k b_\nu + c^+_{k-\nu}c_k b^+_\nu]$$

$$= \sum_{k,\nu} C_{eL}\vec{a}\cdot\vec{k}[c^+_{k+\nu}c_k b_\nu + c^+_{k-\nu}c_k b^+_\nu], \tag{2}$$

$$H_{eh} = \sum_{k,w,j} \frac{e^2}{\varepsilon j^2}[c^+_{k+j}c_k d^+_{w-j}d_w + c^+_{k-j}c_k d^+_{w+j}d_w]$$

$$= \sum_{k,w,j} C_{eh}[c^+_{k+j}c_k d^+_{w-j}d_w + c^+_{k-j}c_k d^+_{w+j}d_w], \tag{3}$$

$$H_{ep} = \sum_{k,q} C_{ep}(c^+_{k+q}c_k b_q - c^+_{k-q}c_k b^+_q). \tag{4}$$

Here H_{eL}, H_{eh}, and H_{ep} are electron-photon, unscreened electron-hole, and electron-phonon interaction, respectively. $\vec{a}$ is unit vector of laser vector potential $\vec{A}, \varepsilon_\nu, \varepsilon$ are the optical and static dielectric constant of fused silica, c^+_k, c_k (d^+_w, d_w, b^+_ν, b_ν, and b^+_q, b_q) are the creation and annihilation operator of an electron (hole, photon, and phonon), and $\vec{k}$, $\vec{w}$, $\vec{q}$, and $\vec{\nu}$ are the wave vector of an electron, hole, phonon, and photon, respectively. m is the CBE effective mass, ω_ν is the frequency of the laser, and $\vec{j}$ is the transfer of $\vec{k}$ in the process of electron-hole scattering. For a LO phonon, the constant is $C^{(o)}_{ep} = ie/q(\hbar\omega_{\rm LO}/2\varepsilon_p)^{1/2}$,[20–22] where $1/\varepsilon_p = 1/(\varepsilon_\nu - \varepsilon)$. There are two dominant LO-phonon modes with phonon energies $\hbar\omega_{\rm LO}$ of 63 and 153 meV in fused silica, and the values of $\varepsilon_0/\varepsilon_p$ are 0.063 and 0.143, respectively.[5,20,25] For an acoustic phonon, the constant is $C^{(a)}_{ep} = iCq(\hbar/2\rho\omega_q)^{1/2}$, where ω_q is the phonon frequency, and the density of fused silica is $\rho = 2.2\times10^3$ kg/m^3. The deformation-potential constant C varies from 6 eV at low kinetic energy of CBE to about 2 eV at high energies.[5,20–22]

The transition element of the second-order perturbation process can be written as[23,24]

$$S = \sum_n \frac{\langle f|H|n\rangle\langle n|H|i\rangle}{E_i - E_n}, \tag{5}$$

where $|i\rangle$, $|f\rangle$, and $|n\rangle$ are initial, final, and intermediate states, and E_i, E_n are energies of the initial and intermediate states, respectively. The formula of transition rates is[23]

$$W = \int \frac{2\pi}{\hbar}|S|^2\delta(E_f - E_i)dS_f. \tag{6}$$

Now we calculate the linear absorption rates of CBE scattered simultaneously by a hole. Integrating over the final states S_f in Eq. (6) is equivalent to a sum over $\vec{j}$. It is in the range $j_{\rm min} \leqslant j \leqslant j_{\rm max}$ due to the energy and momentum conservation,[23] where $j_{\rm min}$ and $j_{\rm max}$ are

$$\frac{j_{\pm\,\rm min}}{k} = \left(1 + \frac{\hbar\omega_\pm}{E}\right)^{1/2} - 1 \tag{7}$$

$$\frac{j_{\pm\,\rm max}}{k} = \left(1 + \frac{\hbar\omega_\pm}{E}\right)^{1/2} + 1, \tag{8}$$

where the sign $+$ and $-$ denote that CBE momentum increases or decreases by j in the transition process. In fused silica, the effective mass of an electron at the bottom of the conduction band is about $0.5m_e$, and it approaches m_e at high kinetic energies,[20–22] where m_e is the mass of a bare electron. In contrast, the hole mass at the top of valence band is about $5-10m_e$.[21] Since the effective mass of the hole is

much larger than that of CBE, the energy transfer of the hole in the process of photon-electron-hole interaction is much less than that of the electron and can be neglected. Here the total change of CBE kinetic energy $\hbar\omega_{\pm}$ is approximately equal to $\hbar\omega_{\nu}$.

In the present study, we assume the holes that take part in the photon absorption process are mainly produced by multiphoton ionization. Because this process takes place principally at the peak of the pulse,[6–8] the holes will effect the total processes of CBE heating and avalanche. Since the hole density generated by impact ionization is not high enough to contribute significantly to the CBE heating until late in the pulse, we neglect its effects.

Integrating Eq. (6), we obtain the hole-assisted linear absorption rates of CBE,

$$W_{\pm}=\frac{e^6\hbar^2\eta_{\nu}FN_h}{64\sqrt{2}\pi\varepsilon_{\nu}\varepsilon^2(\hbar\omega_{\nu})^4c\sqrt{m^3E}}\times\left\{(3\cos^2\beta-1)x^2+8[1-\cos^2\beta-g(3\cos^2\beta-1)]\times\ln\left(\frac{j_{\pm\max}}{j_{\pm min}}\right)-4g^2(3\cos^2\beta-1)x^{-2}\right\}. \tag{9}$$

Here we definine $x_{\pm\max}=j_{\pm\max}/k$, $x_{\pm\min}=j_{\pm\min}/k$, $x^i=x^i_{\pm\max}-x^i_{\pm\min}$, $i=-2,0,2,4,6,\ldots$, and $g=(\hbar\omega_{\pm})/(2E)$. E is the kinetic energy of CBE in the initial state, β is the angle between $\vec{A}$ and $\vec{k}$, c is the light velocity, N_h is the hole concentration, F is the laser intensity, and η_{ν} is the refractive index in fused silica.[26]

Substituting H_{ep} with H_{eh}, we can get the acoustic phonon-assisted one-photon absorption rates[5]

$$W_{\pm}=\frac{e^2C^2k_BT\eta_{\nu}F(2mE^3)^{1/2}}{192\pi\varepsilon_{\nu}(\hbar\omega_{\nu})^4\hbar^2\rho v_s^2c}\times\{4x^4+(3\cos^2\beta-1)[x^6\mp6(g\pm\tfrac{1}{3})x^4+12g^2x^2]\}, \tag{10}$$

where V_s is the sound velocity in fused silica,[21] the range of phonon wave vector is the same as Eqs. (7) and (8) but the $\hbar\omega_{\pm}$ is equal to $\hbar\omega_{\nu}\pm\hbar\omega_{q_5}$. For the LO phonon, the absorption rates can be written as[5]

$$W_{\pm}=\frac{e^4\hbar\omega_{\mathrm{LO}}E^{1/2}\eta_{\nu}F}{128\sqrt{2}\pi\varepsilon_{\nu}\varepsilon_p m^{1/2}c(\hbar\omega_{\nu})^4}\begin{pmatrix} n(\omega_{\mathrm{LO}}) \\ n(\omega_{LO})+1\end{pmatrix}\left\{\tfrac{16}{3}x^2+(3\cos^2\beta-1)\left[x^4\mp8(g\pm\tfrac{1}{3})x^2+16g^2\ln\left(\frac{q_{\pm\max}}{q_{\pm\min}}\right)s\right]\right\}, \tag{11}$$

where $n(\omega_{\mathrm{LO}})$ is the LO-phonon occupation number for phonon absorption and the occupation number $n(\omega_{\mathrm{LO}})+1$ for phonon emission.

We calculate all the one-photon absorption rates for various hole concentration, laser intensity, and wavelengths and at all possible values for the angle between the laser field and electron momentum. The dependence of one-photon absorption rates on the kinetic energy of CBE is plotted in Fig. 1 and Fig. 2, where wavelengths λ are 526 nm and 248 nm,

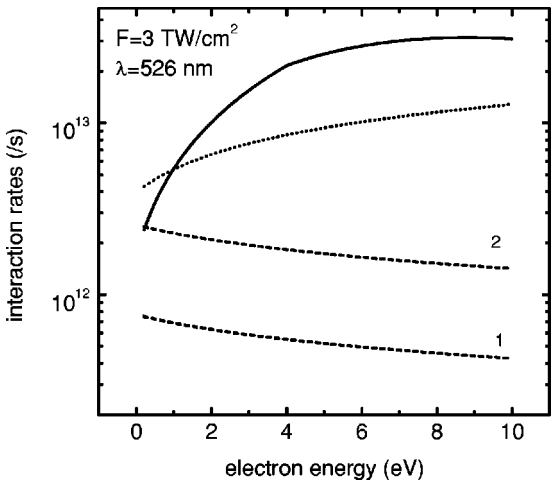

FIG. 1. The one-photon absorption rates as a function of the CBE kinetic energy. The solid and the dotted curves indicate the rates that CBE is scattered by an acoustic phonon and a LO phonon, and the dashed curves of 1 and 2 indicate the rates that CBE scatters off a hole as $N_h=3\times10^{19}$ and $10^{20}/\mathrm{cm}^3$, respectively.

respectively. Here laser intensity F is taken as 3 TW/cm^2, and the electron crystal momentum is parallel to the laser vector potential, namely, $\beta=0$. The solid and the dotted curves indicate the rates for the acoustic phonon and the LO-phonon-assisted process, respectively. The two dashed curves of 1,2 in Fig. 1 are for the hole-assisted process for $N_h=3\times10^{19}/\mathrm{cm}^3$ and $10^{20}/\mathrm{cm}^3$, and the corresponding pulse widths can be calculated to be about 1 ps and 3.5 ps.[7] In Fig. 2, the two dashed curves are for $N_h=5\times10^{20}/\mathrm{cm}^3$, and $10^{21}/\mathrm{cm}^3$, and the pulse widths are 0.8 ps and 2 ps, respectively. These results show that the hole-assisted one-photon absorption rates of CBE at visible light laser radiation gradually approach those of the phonon-assisted process as CBE kinetic energies decrease (see Fig. 1), while for uv lasers, they can exceed those for the phonon-assisted process, and the hole-assisted process becomes dominant.

We have also investigated the linear absorption processes of CBE due to impurity scattering and piezoelectric scatter-

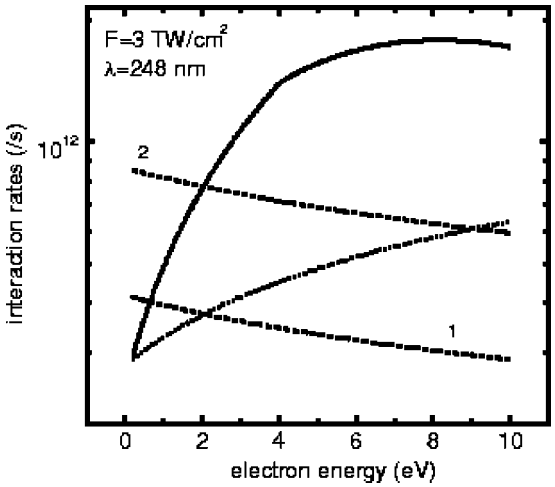

FIG. 2. The one-photon absorption rates as a function of the CBE kinetic energy. The legends are the same as Fig. 1 except for $N_h=5\times10^{20}$ and $10^{21}/\mathrm{cm}^3$ here.

ing. The theoretical results indicate the rates of energy gains are about 1% of those of the phonon-assisted process.

III. THIRD-ORDER PERTURBATION THEORY

The transition element of two-photon absorption is

$$S=\sum_{n,m}\frac{\langle f|H|m\rangle\langle m|H|n\rangle\langle n|H|i\rangle}{(E_i-E_n)(E_i-E_m)}. \tag{12}$$

There are three different orders in these processes for one phonon absorbed (+) or emitted (−) first, second, and third. The intermediate states of the first order can be written as

$$\begin{aligned}|n1\rangle&=|\vec{k}\pm\vec{q},n_q\mp1,n_\nu\rangle,\\ |m1\rangle&=|\vec{k}\pm\vec{q},n_q\mp1,n_\nu-1\rangle.\end{aligned} \tag{13}$$

For the other two orders, the intermediate states can be written out similarly.

Inserting Eq. (13) into Eq. (12), and summing over all three transition elements, we obtain the square of the total element,

$$|S|^2=\frac{|C_{ep}|^2|C_{eL}|^4n_qn_\nu(n_\nu-1)}{(\hbar\omega_\nu)^4}(\vec{a}\cdot\vec{q})^4. \tag{14}$$

Based on Eqs. (6) and (12), after tedious integration similar to that of the second-order perturbation theory, the acoustic phonon-assisted two-photon absorption rates of CBE can be derived to be

$$W_\pm=M\times[\cos^4\beta G^{(1)}+\tfrac{3}{8}\sin^4\beta G^{(2)}+3\sin^2\beta\cos^2\beta G^{(3)}]. \tag{15}$$

Here M and $G^{(i)}(i=1,2,3)$ are

$$M=\frac{e^4C^2k_BT\eta_\nu^2F^2E^{5/2}}{2\sqrt{2m}\pi\varepsilon_\nu^2(\hbar\omega_\nu)^8\rho v_s^2c^2}, \tag{16}$$

$$G^{(1)}=\frac{1}{2}g^4x^2-\frac{1}{2}g^3x^4+\frac{1}{4}g^2x^6-\frac{1}{16}gx^8+\frac{1}{160}x^{10}, \tag{17}$$

$$G^{(2)}=\frac{1}{2}g^4x^2-\frac{1}{2}(1+g)g^2x^4+\frac{1}{6}\left((1+g)^2+\frac{1}{2}g^2\right)x^6-\frac{1}{16}(1+g)x^8+\frac{1}{160}x^{10}, \tag{18}$$

$$G^{(3)}=-\frac{1}{2}g^4x^2+\frac{1}{4}(1+2g)g^2x^4-\frac{1}{6}\left(g+\frac{3}{2}g^2\right)x^6+\frac{1}{32}(1+2g)x^8-\frac{1}{160}x^{10}. \tag{19}$$

Here the definitions of $x_{\pm\max}$, $x_{\pm\min}$, and g are similar to the case of one-photon absorption, but the total change of CBE kinetic energy $\hbar\omega_\pm$ is equal to $2\hbar\omega_\nu\pm\hbar\omega_q$.

For the LO phonon, the formula of two-photon absorption rates is similar to Eq. (15), however M and G are different,

$$M=\frac{e^6(\hbar\omega_{\rm LO})\hbar^2\eta_\nu^2F^2E^{3/2}}{4\sqrt{2}\pi(\hbar\omega_\nu)^8m^{3/2}\varepsilon_\nu^2\varepsilon_pc^2}, \tag{20}$$

$$G^{(1)}=g^4\ln\left(\frac{x_{\pm\max}}{x_{\pm\min}}\right)-g^3x^2+\frac{3}{8}g^2x^4-\frac{1}{12}gx^6+\frac{1}{128}x^8, \tag{21}$$

$$G^{(2)}=g^4\ln\left(\frac{x_{\pm\max}}{x_{\pm\min}}\right)-(1+g)g^2x^2+\frac{1}{4}\left((1+g)^2+\frac{1}{2}g^2\right)x^4-\frac{1}{12}(1+g)x^6+\frac{1}{128}x^8, \tag{22}$$

$$G^{(3)}=-g^4\ln\left(\frac{x_{\pm\max}}{x_{\pm\min}}\right)+\frac{1}{2}(1+2g)g^2x^2-\frac{1}{4}\left(g+\frac{3}{2}g^2\right)x^4+\frac{1}{24}(1+2g)x^6-\frac{1}{128}x^8. \tag{23}$$

For unscreened electron-hole scattering, M and G are

$$M=\frac{e^8N_h\eta_\nu^2F^2\sqrt{E}}{4\sqrt{2}\pi\hbar^4\omega_\nu^8\varepsilon_\nu^2m^{5/2}\varepsilon_<^2c^2}, \tag{24}$$

$$G^{(1)}=-\frac{1}{2}g^4x^{-2}-2g^3\ln\left(\frac{x_{\pm\max}}{x_{\pm\min}}\right)+\frac{3}{4}g^2x^2-\frac{1}{8}gx^4+\frac{1}{96}x^6, \tag{25}$$

$$G^{(2)}=-\frac{1}{2}g^4x^{-2}-2(1+g)g^2\ln\left(\frac{x_{\pm\max}}{x_{\pm\min}}\right)+\frac{1}{2}\left((1+g)^2+\frac{1}{2}g^2\right)x^2-\frac{1}{2}(1+g)x^4+\frac{1}{96}x^6, \tag{26}$$

$$G^{(3)}=\frac{1}{2}g^4x^{-2}+(1+2g)g^2\ln\left(\frac{x_{\pm\max}}{x_{\pm\min}}\right)-\frac{1}{2}\left(g+\frac{3}{2}g^2\right)x^2+\frac{1}{16}(1+2g)x^4-\frac{1}{96}x^6, \tag{27}$$

where $\hbar\omega_\pm=2\hbar\omega_\nu$.

The two-photon absorption rates are shown in Figs. 3 and 4 for wavelengths of 526 nm and 248 nm, respectively. Comparing Fig. 3 with Fig. 1, we find that the rates of energy gains by CBE in the acoustic phonon-assisted two-photon process are nearly equal to those of the corresponding linear absorption for 526 nm, while for 248 nm, it is about 10% of those of the linear process. With the increase of the laser intensity, the phonon-assisted nonlinear absorption will become more and more important.

The two-photon absorption rates of CBE in LO-phonon- and hole-assisted processes are much less than those of the corresponding linear processes. This is because both the one- and the two-photon absorption rates are proportional to the square of scattering elements of electron-phonon or electron-hole interaction, $W\propto|S|^2$. The wave vector of phonon $\vec{q}$ or the change of hole wave vector $\vec{j}$ in two-photon processes is larger than those of the one-photon processes. The acoustic

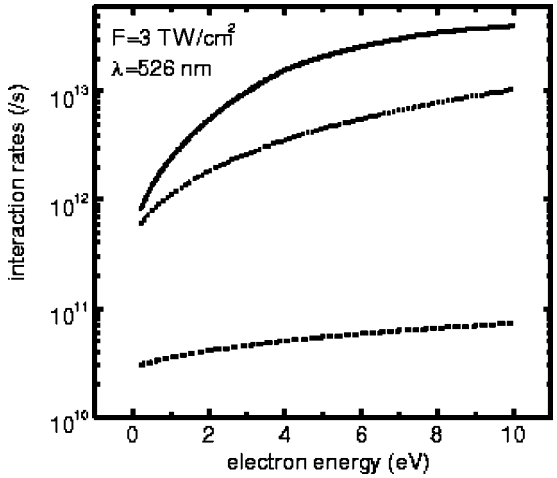

FIG. 3. The two-photon absorption rates as a function of CBE kinetic energy. The solid, dotted, and dashed curves indicate the absorption rates by CBE scattered by an acoustic phonon, a LO phonon, and a hole as $N_h=3\times10^{19}/\mathrm{cm}^3$, respectively.

phonon-electron scattering element is independent of phonon wave vector, but for LO-phonon and electron-hole scattering, they are inversely proportional to the wave vector q and j^2, respectively.

The total absorption rates and the linear absorption rates for CBE in the acoustic and LO-phonon-assisted process are illustrated in Fig. 5. If the CBE-hole scattering and nonlinear absorption are considered, the rates of energy gain by CBE from the laser field will be enhanced by approximately a factor of 2.

IV. DISCUSSION

Optical breakdown and thermal damage are proposed as two kinds of LID mechanisms.[4–15] Which one is the dominant process depends on the laser intensity, via the rates of CBE energy gain from the laser field and the rates of their kinetic energy loss to the lattice.[4–7] The electron-phonon interaction in fused silica has been studied experimentally and

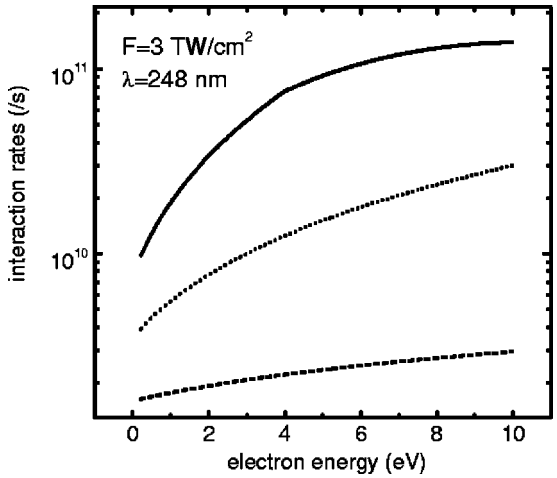

FIG. 4. The two-photon absorption rates as a function of CBE kinetic energy. The solid, dotted, and dashed curves indicate the absorption rates by CBE scattered by an acoustic phonon, a LO phonon, and a hole as $N_h=5\times10^{20}/\mathrm{cm}^3$, respectively.

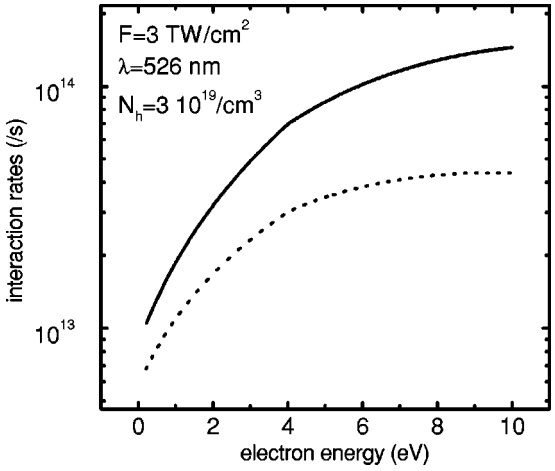

FIG. 5. Comparison of the total absorption rates (solid curve) with those of the linear absorption (dotted curve) for only a phonon is considered. Here $N_h=3\times10^{19}/\mathrm{cm}^3$.

theoretically,[20,21] hence the rates of energy transfer to the lattice by CBE can be easily estimated. Initially, all the electrons stay near the bottom of the conduction band. As proposed in Refs. 6 and 7, the condition for avalanche dominant regimes can be presented as

$$W_{\text{one-tot}}\times\hbar\omega_\nu+W_{\text{two-tot}}\times(2\hbar\omega_\nu)|_{E\to0}=W_{ph}\times\hbar\omega_\nu|_{E\to0}, \tag{28}$$

where $W_{\text{one-tot}}$, $W_{\text{two-tot}}$, and W_{ph} are the one-photon absorption rates, two-photon absorption rates, and the rates of electron-phonon interaction, respectively. The dependence of bounding intensity on the photon energy and the hole density is shown in Fig. 6. Here the thin solid curve, the thick solid, and the dotted and the dashed curve represent the results for phonon-assisted linear absorption and for the total absorption for $N_h=0$, $10^{20}/\mathrm{cm}^3$, and $5\times10^{20}/\mathrm{cm}^3$, respectively. Figure 6 shows that the process of two-photon absorption reduces the bounding intensity of fused silica at visible light laser

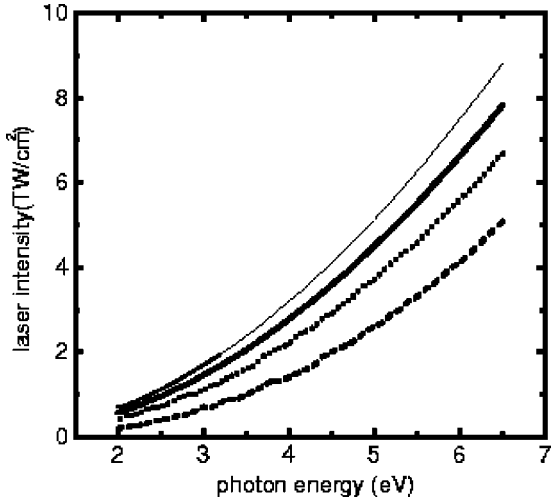

FIG. 6. The dependence of bounding laser intensity on photon energy. The thin solid curve indicates the intensity for which only the linear absorption by CBE scattered by a phonon is considered, and the thick solid, dotted, and dashed curves indicate that total absorption is considered for $N_h=0,10^{20}/\mathrm{cm}^3$, and $5\times10^{20}/\mathrm{cm}^3$, respectively.

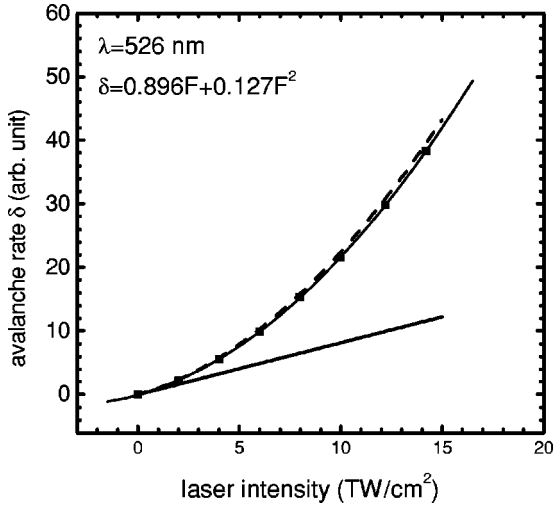

FIG. 7. The dependence of the avalanche rates on laser intensity and hole density. The thick line indicates that only the linear absorption by CBE scattered by a phonon is considered; the squares and the dashed curve, indicate that total absorption is considered for $N_h=0$, and $5\times10^{19}/\mathrm{cm}^3$, respectively. The thin solid line is a numerical simulation.

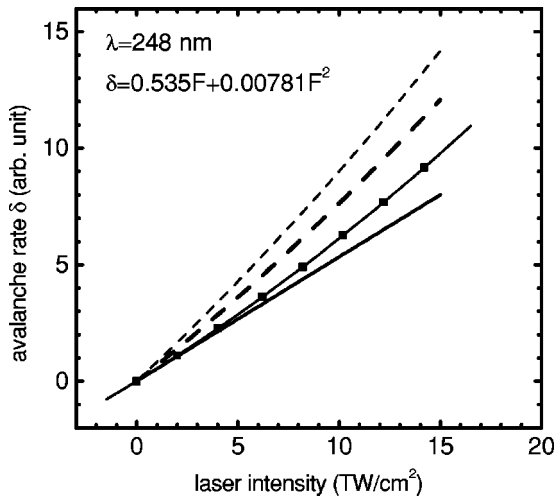

FIG. 8. The dependence of the avalanche rates on laser intensity and hole density. The legend is the same as that in Fig. 7 except for $N_h=5\times10^{20}$ and $10^{21}/\mathrm{cm}^3$ for the dashed and the dotted curves.

radiation by about one-third. But for an uv laser, the effects of these processes are not important. This is because the rates of two-photon absorption of CBE in an uv laser field are much less than those of a visible laser (see Figs. 1 and 3 and Figs. 2 and 4). However, because the hole density generated by multiphoton ionization for an uv laser is much higher than that of a visible laser, then if the hole-assisted absorption of CBE is considered, the uv laser bounding intensity will be strongly reduced and approach that of a visible laser. For example, the experimental value of the bounding intensity of fused silica under 526 nm laser radiation is in the range of 0.7–0.4 TW/cm^2.[6,7] We find it will lower from 0.9 TW/cm^2 to 0.7 TW/cm^2 if total absorption is considered for $N_h=0$, which corresponds well with the experimental results.

It has been presented that the avalanche rate δ is proportional to the laser intensity. In the flux-doubling formulation, δ can be shown as[7]

$$\delta=pL^2\Big/\int_0^{E_g}\frac{dE}{\sigma(E)}=\alpha_1 F, \tag{29}$$

where p and α_1 are constants, $\sigma(E)L^2$ is the rate of energy gain of CBE given by the classical method, E_g is the band gap of solids, and L is the electric intensity of a laser field. The linearity between δ and the laser intensity is correct if *only* linear absorption is considered. It is not so when the nonlinear absorption and the hole-assisted absorption are included. The dependence of δ on laser intensity and hole density is shown in Figs. 7–9. The line in Fig. 7 is the numerical results in which only the phonon-assisted linear process is considered. The squares and the dashed curve are the results for total absorption for $N_h=0$ and $5\times10^{19}/\mathrm{cm}^3$. In Fig. 7, the laser wavelength is 526 nm. The avalanche rate for 248 nm laser radiation is shown in Fig. 8. Under visible wavelength laser radiation, the avalanche rate is greatly enhanced by the nonlinear absorption, and so does it by the hole-assisted linear process for the case of uv laser radiation.

The rates of hole-assisted two-photon absorption are very small (see Figs. 3 and 4) and may be neglected. Then we get the linear dependence of δ at 526 nm laser radiation on hole density N_h, as shown in Fig. 9 for $F=3$ TW/cm^2 and 5 TW/cm^2. The dependence of δ on N_h for a 248 nm laser is the same as that of 526 nm and is omitted. Because $\delta\propto F$ if only linear absorption is considered, we can guess, therefore, that δ should include the term FN_h on the basis of Eq. (9). Moreover, in Fig. 7 and Fig. 8, we imitate the value of avalanche rate for $N_h=0$ with $\delta=0.896F+0.127F^2$ for 526 nm and $\delta=0.535F+0.00781F^2$ for 248 nm, respectively. This observation suggests that δ may be written as

$$\delta=\alpha_1 F+\alpha_2 F^2+\alpha_3 F N_h, \tag{30}$$

where α_2 and α_3 are constants.

The CBE generation processes have been investigated theoretically.[5,9,16] It was proposed that the avalanche rates

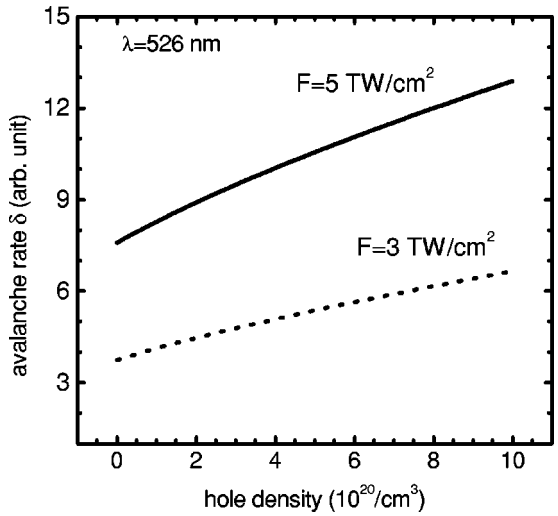

FIG. 9. The relation of avalanche rates with hole density.

decreased dramatically as the laser wavelengths became shorter, and then multiphoton absorption becomes the dominant mechanism for CBE generation at visible wavelengths. However, under ultrashort pulse laser radiation, δ is enhanced significantly, as indicated by our study, by phonon-assisted nonlinear absorption and hole-assisted linear absorption. Then we propose that at visible wavelengths, the avalanche is the dominant mechanism of CBE generation in wide-gap materials. Even at uv wavelengths, it is also a non-neglectable process. For example, under 526 nm laser radiation for pulse width $\tau=0.5$ ps and peak power $F_0=4$ TW/cm^2, the avalanche rates will increase by 60% if the nonlinear absorption and the hole-assisted linear absorption are also included in the calculations. Then we obtain that the CBE density generated by impact ionization is four times larger than that generated by multiphoton absorption, and it contributes more than 80% to the total CBE concentration.

The present study shows that the avalanche rate should be as shown in Eq. (30) instead of Eq. (29), and this will lead to a different estimation on the damage threshold. Following Ref. 7, the damage threshold I_{pl} for only phonon-assisted linear absorption being considered is

$$I_{pl}=\frac{2}{\alpha_1}\ln\left(\frac{n_c}{n_0}\right), \tag{31}$$

where n_0 is CBE density generated by multiphoton absorption, and n_c is the critical CBE density when optical breakdown takes place. By substituting δ from Eq. (29) with Eq. (30), we can obtain the damage threshold I_{tot} for total absorption processes being considered. Then the ratio can be written as

$$\frac{I_{\mathrm{tot}}}{I_{pl}}=\frac{\alpha_1}{\alpha_1+\alpha_3 N_h+(\alpha_2 F_0)/\sqrt{2}}, \tag{32}$$

where F_0 is the peak power. For example, under 526 nm laser radiation for pulse width $\tau=1$ ps, the damage threshold I_{pl} are calculated to be about 1.5 J/cm^2. Then from Eq. (32) we get that I_{tot} should be 1.3 J/cm^2. This value agrees excellently with experimental results.[7] With the decrease of laser pulse widths, both the peak power of the damage threshold and CBE density generated by multiphoton absorption will increase, therefore the damage threshold I_{tot} will be reduced more significantly.

V. CONCLUSION

In conclusion, we calculate the one-photon and the two-photon absorption rates of CBE by perturbation theory, where the laser field is treated as a quantum field. When the laser intensity is of the order of TW/cm^2, we find that besides phonon-assisted linear absorption, hole-assisted linear absorption and phonon-assisted two-photon absorption are also very important for CBE heating. The avalanche rate thus increases greatly, and impact ionization becomes the dominant mechanism of CBE generation under visible light laser radiation. It is also an important process of CBE generation for uv laser radiation. The present result gives a lower damage threshold (by approximately a factor of 0.15 as pulse width is 1 ps) than previously calculated ones. The damage threshold continues to decrease as the laser pulse duration is decreased. It should be pointed out that our calculation methods are suitable for common optically transparent materials. If knowledge about their energy bands, phonon states, and electron-phonon scattering rates is available, their damage mechanism can be investigated similarly.

ACKNOWLEDGMENTS

This work was supported by the National High-Tech ICF Committee in China.

*Electronic address: Jiatq@263.net

[1] H. Varel, D. Ashkenzai, A. Rosenfeld, M. Wahmer, and E.E.B. Campbell, Appl. Phys. A: Mater. Sci. Process. **65**, 367 (1997).
[2] X. Liu, D. Du, and G. Mourou, IEEE J. Quantum Electron. **33**, 1706 (1997).
[3] J. Zhang *et al.*, Phys. Rev. Lett. **74**, 1335 (1995).
[4] M. Sparks *et al.*, Phys. Rev. B **24**, 3519 (1981).
[5] D. Arnold and E. Cartier, Phys. Rev. B **46**, 15 102 (1992).
[6] B.C. Stuart, D. Feit, A.M. Rubenchik, B.W. Shore, and M.D. Perry, Phys. Rev. Lett. **74**, 2248 (1995).
[7] B.C. Stuart, D. Feit, A.M. Rubenchik, B.W. Shore, and M.D. Perry, Phys. Rev. B **53**, 1749 (1996).
[8] M.H. Niemz, Appl. Phys. Lett. **66**, 1181 (1995); F. Bonneau and B. Cazalis, SPIE. (Bellingham, WA, 1996), Vol. 2714, pp. 650–659; Haiwu Yu and Shaoxian Meng, J. Appl. Phys. **81**, 85 (1997).
[9] S.C. Jones and P.E. Braunlich, Opt. Eng. **28**, 1039 (1989).
[10] J. Ihlemann, B. Wolf, and P. Simon, Appl. Phys. A: Solids Surf. **54**, 363 (1992); S. Papernov and A.W. Schmid, J. Appl. Phys. **82**, 5422 (1997); A. Kar and J. Mazumder, *ibid.* **68**, 3884 (1990); M. Reichling, A. Bodemann, and N. Kaiser, Thin Solid Films **320**, 264 (1998).
[11] D. Du, X. Liu, G. Korn, J. Squier, and G. Mourou, Appl. Phys. Lett. **64**, 3071 (1994).
[12] M. Lenzner *et al.* Phys. Rev. Lett. **80**, 4076 (1998).
[13] K. Yoshida, H. Yoshida, T. Kamimura, and N. Kuzuu, Jpn. J. Appl. Phys., Part 1 **37**, 1882 (1998).
[14] J. Kruger and W. Kautek, Appl. Surf. Sci. **96-98**, 430 (1996); H. Varel *et al.*, Appl. Phys. A: Mater. Sci. Process. **62**, 293 (1996); D. Linde, K. Sokolowski-Tinten, and J. Bialkowski, Appl. Surf. Sci. **109/110**, 1 (1997).
[15] F. Chen and S.X. Meng, Prog. Phys. **18**, 187 (1998) (in Chinese); T.Q. Jia *et al.*, High Power Laser Particle Beams **10**, 375 (1998) (in Chinese).
[16] B. Gorshkov, A. Epifanov, and A. Manenkov, Zh. Éksp. Teor. Fiz. **76**, 617 (1979) [Sov. Phys. JETP **49**, 309 (1979)].
[17] P. Simon, H. Gerhardt, and S. Szatmart, Opt. Lett. **14**, 1207 (1989); T. Mizunami and K. Takagi, *ibid.* **19**, 463 (1994).
[18] V. Nathan, A.H. Guenther, and S.S. Mitra, J. Opt. Soc. Am. **2**, 294 (1985).
[19] L.V. Keldysh, A.H. Guenther, and S.S. Mitra, Zh. Éksp. Teor. Fiz. **47**, 1945 (1964) [Sov. Phys. JETP **20**, 1307 (1965)].
[20] M.V. Fischetti, Phys. Rev. Lett. **53**, 1755 (1984); M.V. Fischetti, D.J. DiMaria, S.D. Brorson, T.N. Theis, and J.R. Kirtley, Phys. Rev. B **31**, 8124 (1991).

[21] C. Cartier and F.R. McFeely, Phys. Rev. B **44**, 10 689 (1991).
[22] J.R. Chelidowsky and M. Schluter, Phys. Rev. B **15**, 4020 (1977).
[23] B.K. Ridly, *Quantum Processes in Semiconductors* (Clarendon, Oxford, 1988).
[24] H. Haken, *Quantum Field Theory of Solids* (North-Holland Pub. Co., New York, 1976).
[25] W.T. Lynch, J. Appl. Phys. **43**, 3274 (1972).
[26] J.Z. Li *et al.*, *Optical Handbook* (Shanxi Sci-Tech. Press, Xi'an, 1986) (in Chinese).